Oxidation of ethylbenzene to acetophenone by a Mn catalyst supported on a modified nanosized SiO_2/Al_2O_3 mixed-oxide in supercritical carbon dioxide

M. Arshadi [a], M. Ghiaci [a,*], A. Rahmanian [a], H. Ghaziaskar [a], A. Gil [b]

[a] Department of Chemistry, Isfahan University of Technology, Isfahan, 8415683111, Iran
[b] Department of Applied Chemistry, Los Acebos Building, Public University of Navarra, Campus of Arrosadia, E-31006, Pamplona, Spain

ABSTRACT

The selective oxidation of ethylbenzene to acetophenone with *tert*-butyl hydroperoxide in the presence of an SiO_2/Al_2O_3-supported manganese catalyst occurs with a conversion of 91% and a selectivity of 98%, *in the absence of an organic solvent*, in supercritical carbon dioxide. The catalysts could be reused at least eight times without significant loss of activity. This procedure simplifies the isolation of the reaction products and has the advantage of using only carbon dioxide as a solvent under mild conditions. The electrochemical data for Mn nanocatalysts immobilized at the surface of multi-walled carbon nanotubes were also studied. The results indicate that the Mn catalysts anchored on the modified SiO_2/Al_2O_3 mixed-oxide via 2-aminoethyl-3-aminopropyltrimethoxysilane (2-AE-3-APTMS) have an easily oxidizable environment, lower oxidation potential and lower charge-transfer resistance, thus leading to a higher catalytic activity and selectivity than when 3-aminopropyltrimethoxysilane (3-APTES) is used.

© 2012 Elsevier B.V. All rights reserved.

1. Introduction

Selective oxidation of the C—H bonds in ethylbenzene is an attractive field and remains an unsolved problem in chemistry as reaction intermediates such as acetophenone are more susceptible to further oxidation than the corresponding carboxylic acid, thus lowering the selectivity and making highly selective ketone formation more difficult. The selective production of acetophenone would provide high added value as this compound is used as an intermediate for the manufacture of pharmaceuticals, resins, alcohols, esters, aldehydes and tear gas, and is also used as a component in perfumery and as a solvent for cellulose ethers. Production of this ketone has traditionally involved Friedel–Crafts acylation of benzene by an acyl halide or acid anhydride in the presence of stoichiometric quantities of homogeneous Lewis acids (e.g., $AlCl_3$, BF_3, $FeCl_3$, $ZnCl_2$, $SnCl_4$, $TiCl_4$) or strong protic acids (e.g., H_2SO_4, HF), thus leading to the formation of a large volume of toxic and corrosive waste [1]. Although homogeneous catalysts exhibit excellent activity and selectivity, the technical problems encountered in their use, such as the difficulty in product separation, deactivation by formation of μ-oxo dimers, self-aggregation of active sites and formation of other polymeric species, have tended to restrict their industrial application. Heterogeneous catalysts have an advantage in this respect in that the catalyst can be removed at the end of

reaction by simple filtration. In principle, the product is therefore not contaminated by either a transition metal or ligand, and the catalyst can be recycled for subsequent reaction. Furthermore, the conventional use of volatile solvents in a chemical reaction is of ecological and economic concern, with the replacement of volatile organic solvents in the reaction medium being of utmost importance in the field of green chemistry. It is clear that green chemistry requires both the use of environmentally friendly solvents and heterogeneous rather than homogeneous catalysts in order to be able to recover and reuse the catalyst. One strategy that is often used to transform a homogeneous catalyst into its heterogeneous counterpart involves anchoring the active site onto a solid carrier with a large surface area whilst ensuring that the anchoring methodology maintains the intrinsic activity and selectivity of the catalytic center [2–6].

There has recently been increasing interest in the development of heterogeneously catalyzed oxidation reactions in supercritical carbon dioxide ($scCO_2$) [7–13]. $scCO_2$ is an attractive alternative solvent as its critical parameters ($T_c = 31\,°C$ and $P_c = 73.8\,bar$) are moderate and it is readily available, in other words the amount of energy required to generate supercritical carbon dioxide is relatively low. Furthermore, it has a number of well-defined advantages over conventional liquid organic solvents, such as its chemical inertness towards many substances, its non-flammability and the fact that it can be removed by simple depressurization results in its removal. Likewise, its use means that toxic organic liquids are no longer required and its low polarity means that it can be used during the oxidation of weakly polar substrates such as ethylbenzene.

* Corresponding author.
  E-mail address: mghiaci@cc.iut.ac.ir (M. Ghiaci).

The fact that its physical properties can be tuned by varying pressure and temperature may also enable reaction rates and product selectivity to be improved [14,15]. In addition, the phase behavior of the reaction mixtures greatly affects the oxidations in $scCO_2$. This is related to the presence or absence of mass transfer limitation between phases and to the concentration of substrate, oxidant, and catalyst in the phase where the oxidation mainly takes place.

Despite the fact that the chemistry of manganese has received considerable attention due to the fact that this metal is believed to be catalytically active in a variety of metalloenzymes [16–19], to the best of our knowledge there have been no previous reports regarding the efficient and selective oxidation of ethylbenzene to acetophenone by Mn catalysts immobilized on the organo-functionalized mixed-oxide SiO_2/Al_2O_3, especially in the presence of an environmentally friendly and benign solvent such as $scCO_2$. Likewise, although Schiff base ligands can readily be obtained by polycondensation of diamines with additionally functionalized salicylaldehydes, there have been very few studies involving salicylaldehydes functionalized with pyridine groups [20–25].

Herein we report a simple procedure for the preparation of a new type of Mn catalyst immobilized on a functionalized nanosized SiO_2/Al_2O_3 mixed-oxide via three Schiff base ligands, which are covalently bound through two typical linkers with differing flexibility and hydrophobicity (3-aminopropyl and 2-aminoethyl-3-aminopropyl), and their remarkable catalytic activities and excellent selectivity for the catalytic oxidation of ethylbenzene in $scCO_2$ using *tert*-butyl hydroperoxide as the oxidant and in the absence of a reducing agent. Only a few papers concerning the catalytic oxidation of hydrocarbons in the presence of transition metal-based catalysts and absence of a sacrificial co-reductant have been published to date [25,26].

This particular mixed-oxide was chosen on the basis of its properties, such as low thermal expansion and conductivity, low dielectric constant, excellent creep resistance, robust chemical and thermal stability, good high temperature strength and oxidation resistance [27]. The influence of the electrochemical potential and electrochemical behavior of the immobilized Mn nanocatalyst materials on the catalytic activity of the catalysts was also studied by electrochemical methods such as cyclic voltammetry (CV) and electrochemical impedance spectroscopy (EIS).

The green chemistry goals of our research into the heterogeneous catalytic oxidation of ethylbenzene in $scCO_2$ reaction media are numerous but include the replacement of volatile organic solvents with a more environmentally benign reaction medium ($scCO_2$). Likewise, it appears surprising that the main product is acetophenone and that benzoic acid is rarely observed—it is only detected as a very minor by-product in some systems—when using $scCO_2$ as the reaction medium. Finally, the use of heterogeneous Mn catalysts, especially neat substrate, is a subject of considerable interest from an environmental standpoint as losses of both solvent and catalyst on separation often lead to unacceptable levels of waste.

2. Experimental

2.1. Materials

All reagents (A.R.) were purchased from Merck or Fluka and were used without further purification, except for solvents, which were treated according to standard methods. CO_2 was purchased from Isfahan Zam Zam Company. Graphite powder (particle diameter = 0.1 mm) and carbon nanotubes [(>90% MWCNT basis, $d \times l$ = (110–70 nm) × (5–9 μm) (Fluka)] were used as the substrate when preparing the carbon paste electrode used as working electrode (WE).

2.2. Catalyst characterization

Electrochemical measurements were carried out using a Micro-Autolab, potentiostat/galvanostat (μ3AUT70751) connected to a conventional three-electrode cell. A modified multi-walled carbon nanotube paste electrode was used as the working electrode, a platinum wire as the auxiliary electrode, and an Ag/AgCl/KCl electrode as the reference electrode. Electrochemical impedance measurements were carried out in a conventional three-electrode cell powered by an electrochemical system comprising an Autolab (AUT83593) at a frequency range of 0.1–10,000 Hz. The AC voltage amplitude was 5 mV.

2.3. Preparation of the organometallic functionalized nanosized SiO_2/Al_2O_3 mixed-oxide

SiO_2/Al_2O_3 (1/1) was used as the support. The supported Mn catalysts were prepared by the sol–gel method according to the literature and were fully characterized [28–30]. The SiO_2/Al_2O_3 (1:1)-supported 3-aminopropyl was prepared by refluxing 5.2 g of SiO_2/Al_2O_3 (1:1), which had previously been activated at 550 °C for 6 h in air, with 3.5 cm^3 (0.0195 mol) of 3-aminopropyltrimethoxysilane (3-APTES) in dry dichloromethane (100 cm^3) for 24 h. The resulting solid was filtered, washed with methanol and dichloromethane and then dried at 100 °C under vacuum for 6 h. The same reaction conditions were used to functionalize SiO_2/Al_2O_3 (1:1) with 2-aminoethyl-3-aminopropyltrimethoxysilane (2-AE-3-APTMS). The functionalized SiO_2/Al_2O_3 (1:1) mixed-oxides prepared with these two linkers will hereafter be referred to as Si/Al-*pr*-NH$_2$ and Si/Al-*pr*-NH-*et*-NH$_2$.

The appropriate aldehyde or ketone (salicylaldehyde, methyl-2-pyridylketone or pyridine-2-carbaldehyde) was added to a suspension of Si/Al-*pr*-NH$_2$ or Si/Al-*pr*-NH-*et*-NH$_2$ in dry methanol and the mixture refluxed for 24 h to prepare a Schiff base on the surface of the mixed-oxide (a bidentate ligand). The heterogeneous Mn-based catalyst was then obtained by stirring 0.5 g of the hybrid material (Si/Al mixed-oxide-Schiff base ligand) with Mn(OCOCH$_3$)$_2$·4H$_2$O (5.4 mmol), and LiCl (8.5 mmol) in 30 cm^3 of ethanol whilst refluxing for 24 h. The resulting catalyst (brown powder) was filtered, washed with copious amounts of ethanol and methanol and dried under vacuum at 60 °C (Scheme 1). The chemical composition of the catalysts is presented in Table 1.

2.4. General procedure for oxidation of ethylbenzene

Batch reactions in supercritical carbon dioxide were performed in a 10-cm^3 stainless-steel reactor. The reactor was built to allow filling and emptying via sampling valves, which to allow the reaction mixture to be easily isolated from the catalyst. The reactor was heated in an oil bath and the contents stirred at 400 rpm with a magnetically coupled stirrer. The reactor containing weighed amounts of catalyst and reagents (0.05 mg of catalyst, 2.0 mmol of ethylbenzene, 2.0 mmol of 80% TBHP and n-decane as internal standard) was sealed and purged with CO_2, then heated to the desired temperature under continuous stirring. It was then slowly pressurized using an HPLC pump (JASCO, PU-2080-CO_2). The inlet tube was extended to the bottom of the reactor just above a magnetic stir bar. A frit at the outlet prevented the solid catalyst from escaping. When the reaction was finished (after a set period of time) the stirring was ceased, the reactor was gradually depressurized, and the collected reaction mixture was then purged with CO_2. In the next step, the reactor was cooled to room temperature and the excess gases collected in cold ethanol (each reaction was repeated three times and displayed a relative standard deviation of less than 1.04%). The remaining mixture was centrifuged (if the effluent was not

Table 1
Chemical composition of the catalysts.

Catalyst	Elemental analyses (wt.%)[a]		Organic functional group (mmol/g mixed oxides)[b]
	N	Mn	
SiO$_2$/Al$_2$O$_3$ mixed oxides	–	–	–
Si/Al-*pr*-N=salicylaldehyde	3.9	–	2.8
Si/Al-*pr*-N=methyl-2-pyridylketone	4.4	–	3.1
Si/Al-*pr*-N=pyridine-2-carbaldehyde	4.6	–	3.3
Si/Al-*pr*-NH-*et*-N=salicylaldehyde	5.2	–	3.7
Si/Al-*pr*-NH-*et*-N=methyl-2-pyridylketone	6.2	–	4.4
Si/Al-*pr*-NH-*et*-N=pyridine-2-carbaldehyde	5.6	–	4.0
Si/Al-*pr*-N=salicylaldehyde-Mn	3.2	3.9	2.3
Si/Al-*pr*-NH-*et*-N=salicylaldehyde-Mn	4.9	3.2	3.5
Si/Al-*pr*-N=methyl-2-pyridylketone-Mn	3.9	2.0	2.8
Si/Al-*pr*-NH-*et*-N=methyl-2-pyridylketone-Mn	5.7	3.0	4.1
Si/Al-*pr*-N=pyridine-2-carbaldehyde-Mn	4.0	1.7	2.9
Si/Al-*pr*-NH-*et*-N=pyridine-2-carbaldehyde-Mn	4.6	1.4	3.3

[a] Nitrogen was estimated from the elemental analyses. Mn content determined from ICP analysis.
[b] Determined from the N-contents.

completely removed with CO$_2$ purging), the liquid phase diluted to 5 cm^3 and the samples analyzed using a BEIFEN 3420 gas chromatograph fitted with a FID detector and an HP-5 column (length = 30 m and I.D. = 0.25 mm).

The conversion and selectivity were calculated as follows:

$$\text{Conversion}\,(\%) = 100 \times \frac{(\text{mols of ethylbenzene consumed})}{(\text{mols of ethylbenzene introduced})}$$

$$\text{Selectivity}\,(\%) = 100 \times \frac{(\text{mols of product formed})}{(\text{mols of ethylbenzene consumed})}$$

Leaching experiments were carried out in order to prove the heterogeneous character of the reactions. In representative tests, the organometallic functionalized SiO$_2$/Al$_2$O$_3$ mixed-oxide catalysts were hotly filtered, based on the procedure mentioned above, and the Mn content of the filtrate analyzed by atomic absorption spectrophotometry (AAS).
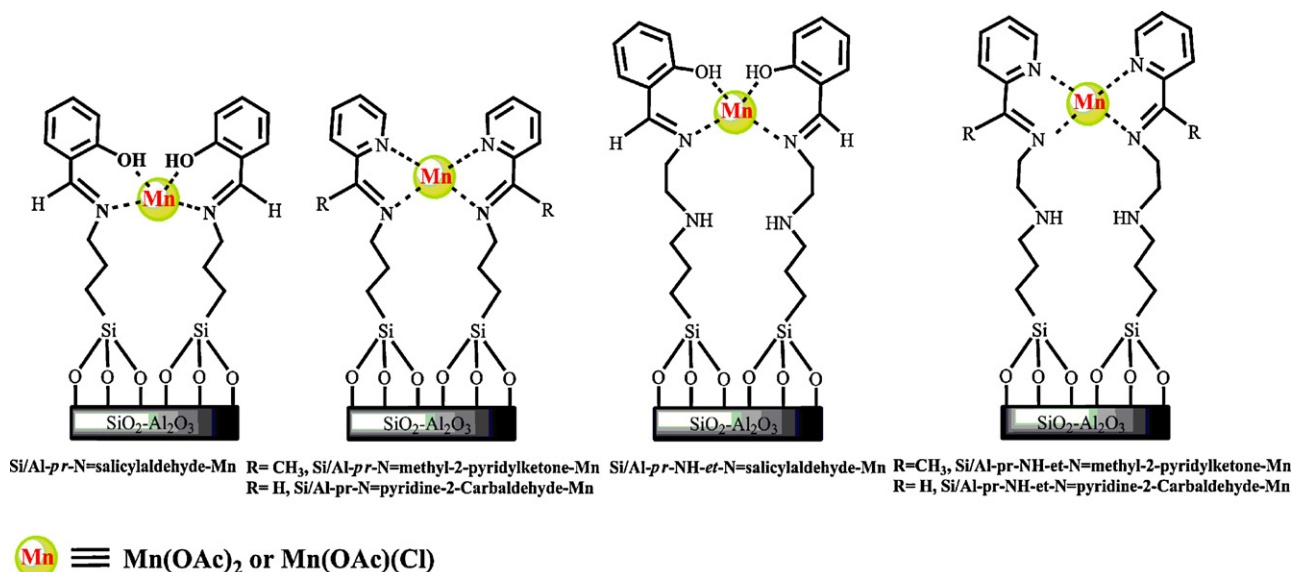
2.5. Preparation of the electrode

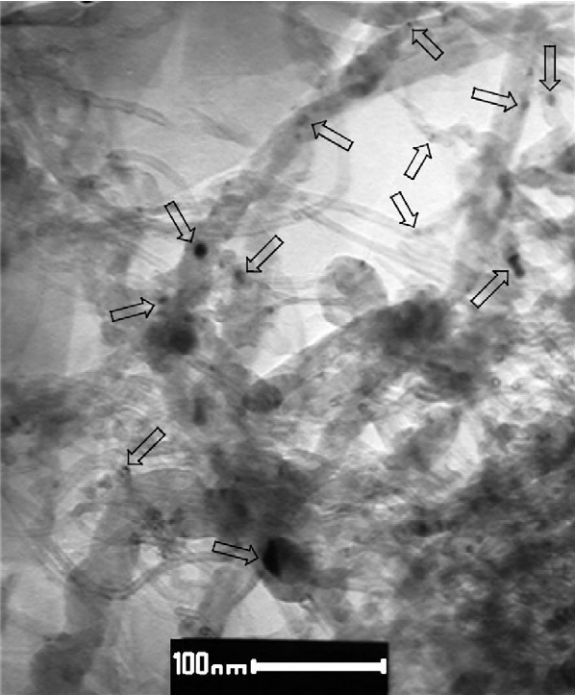A 10-mg sample of the immobilized Mn catalyst was mixed with 79 mg of graphite powder and 10 mg of multi-walled carbon nanotubes in a mortar and pestle (Fig. 1). Then, 0.88 g of paraffin was added using a syringe and the resulting mixture mixed well for 40 min to obtain a uniformly wetted paste. This paste was then packed into a glass tube, and electrical contact was made by pushing a copper wire inside the glass tube into the top of the mixture. When necessary, a new surface was obtained by pushing an excess of the paste out of the tube and polishing it on a weighing paper.

2.6. Recommended procedure for electrochemical analysis

The blend of immobilized Mn catalyst and multiwalled carbon nanotube paste was polished with a clean, white filter paper for electrochemical analysis. To record the cyclic voltammograms for the immobilized Mn catalyst, 10.0 cm^3 of 0.04 mol/dm^3 universal buffer pH 7.0 was transferred into an electrochemical cell and the initial and final potentials adjusted to +0.00 and +1.00 V vs. Ag/AgCl, respectively. The cyclic voltammograms were recorded at a scan rate of 100 mV/s to give the oxidation and reduction signals.

Si/Al-*pr*-N=salicylaldehyde-Mn   R= CH$_3$, Si/Al-*pr*-N=methyl-2-pyridylketone-Mn   Si/Al-*pr*-NH-*et*-N=salicylaldehyde-Mn   R=CH$_3$, Si/Al-pr-NH-et-N=methyl-2-pyridylketone-Mn
R= H, Si/Al-pr-N=pyridine-2-Carbaldehyde-Mn   R= H, Si/Al-pr-NH-et-N=pyridine-2-Carbaldehyde-Mn

Mn ≡ Mn(OAc)$_2$ or Mn(OAc)(Cl)

Scheme 1. Proposed structures of Mn catalysts immobilized on the functionalized SiO$_2$/Al$_2$O$_3$ mixed-oxide.

Fig. 1. TEM micrographs of Si/Al-pr-NH-et-N=methyl-2-pyridylketone-Mn plus carbon nanotube paste electrode (the dark spots are Mn nanoparticles).

3. Results and discussion

3.1. Optimization of experimental parameters

3.1.1. Catalytic oxidation of ethylbenzene over various Mn nanocatalysts

The oxidation of ethylbenzene over Mn catalysts immobilized on the organo-functionalized SiO_2/Al_2O_3 mixed-oxide was first performed at 120 °C in scCO$_2$ (150 bar), with TBHP as oxidant, for

8 h. The results are shown in Table 2. These Mn catalysts were found to be active for oxidation of ethylbenzene to acetophenone in scCO$_2$. The formation of acetophenone (**1**), benzaldehyde (**2**) and benzoic acid (**3**) is shown in Scheme 2; all products were identified by GC–MS. No oxidation at the aromatic ring in ethylbenzene was observed. The catalytic activity of the Mn catalysts was higher when using TBHP as oxidant than when using H_2O_2 (6.5%, entry 8). This may be due to carbon dioxide molecules adsorbed on the surface of the catalysts blocking the access of H_2O_2 to a greater extent than TBHP (stronger oxidant) in supercritical carbon dioxide. However, it may also be due to TBHP being more easily activated upon coordination with the immobilized Mn nanocatalysts than H_2O_2, in other words a coordination stabilizing effect of the surrounding ligands [31]. The H_2O which is added with H_2O_2 can also deactivate active sites and explain the behavior observed. Acetophenone was generally found to be the main product, along with minor quantities of benzaldehyde and benzoic acid.

The selectivity of the various immobilized Mn catalysts studied after 8 h decreased in the order Si/Al-pr-NH-et-N=methyl-2-pyridylketone-Mn (86.0%) > Si/Al-pr-NH-et-N=pyridine-2-carbaldehyde-Mn (84.2%) > Si/Al-pr-N=salicylaldehyde-Mn (83.0%) > Si/Al-pr-N=methyl-2-pyridylketone-Mn (82.1%) > Si/Al-pr-N=pyridine-2-carbaldehyde-Mn (74.6%) > Si/Al-pr-NH-et-N=salicylaldehyde-Mn (69.8%). These findings suggest that the electronic effects of the ligands may increase the selectivity for acetophenone. Indeed, a higher selectivity for acetophenone was achieved when using catalysts containing pyridine rings instead of phenyl rings.
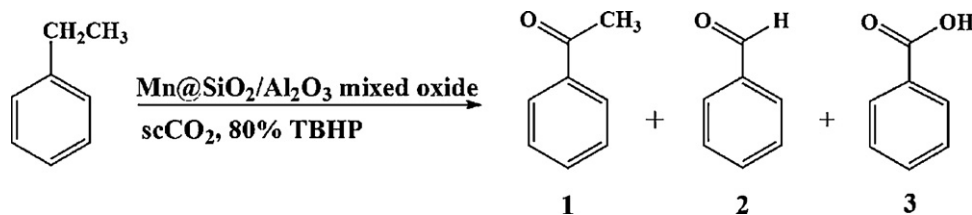
Table 2 also lists the ethylbenzene conversion in scCO$_2$ for the various Mn catalysts. Ethylbenzene conversion for the Mn catalysts immobilized on the organo-functionalized SiO_2/Al_2O_3 mixed-oxide decreased in the order Si/Al-pr-NH-et-N=methyl-2-pyridylketone-Mn (84.0%) > Si/Al-pr-NH-et-N=pyridine-2-carbaldehyde-Mn (67.2%) > Si/Al-pr-NH-et-N=salicylaldehyde-Mn (56.3%) > Si/Al-pr-N=pyridine-2-carbaldehyde-Mn (45.0%) > Si/Al-pr-N=salicylaldehyde-Mn (34.4%) > Si/Al-pr-N=methyl-2-pyridylketone-Mn (33.6%). The reaction was essentially complete after about 8 h, when TBHP efficiency

Table 2
Oxidation of ethylbenzene to acetophenone in the presence of several heterogeneous Mn catalysts in scCO$_2$.

Entry	Catalyst	Ethylbenzene conversion (mol%)	TON[i]	Selectivity (mol%)		
				Ac	Bd	Ba
1	No catalyst	–	–	–	–	–
2	Si/Al-pr-N=salicylaldehyde-Mn	34.4	19.3	83.0	17.0	0
3	Si/Al-pr-NH-et-N=salicylaldehyde-Mn	56.3	38.8	69.8	23.0	7.1
4	Si/Al-pr-N=methyl-2-pyridylketone-Mn	33.6	37.4	82.1	15.4	2.4
5	Si/Al-pr-NH-et-N=methyl-2-pyridylketone-Mn	84.0	62.2	86.0	14.0	0
6	Si/Al-pr-N=pyridine-2-carbaldehyde-Mn	45.0	58.4	74.6	21.8	3.5
7	Si/Al-pr-NH-et-N=pyridine-2-carbaldehyde-Mn	67.2	106	84.2	13.7	2.0
8	Si/Al-pr-N=salicylaldehyde-Mn[a]	6.50	3.64	91.0	9.0	0
9	Si/Al-pr-NH-et-N=methyl-2-pyridylketone-Mn[b]	91.0	67.4	98.1	1.80	0
10	Si/Al-pr-N=salicylaldehyde-Mn[c]	82.5	46.3	95.6	1.80	2.58
11	Si/Al-pr-NH-et-N=methyl-2-pyridylketone-Mn[d]	39.0	29.1	82.0	18.0	0
12	Si/Al-pr-NH-et-N=methyl-2-pyridylketone-Mn[e]	86.7	64.2	88.5	11.5	0
13	Si/Al-pr-NH-et-N=methyl-2-pyridylketone-Mn[f]	51.3	38.0	80.5	5.90	13.3
14	Si/Al-pr-NH-et-N=methyl-2-pyridylketone-Mn[g]	84.0	62.2	87.2	11.3	0
15	Si/Al-pr-NH-et-N=methyl-2-pyridylketone-Mn[h]	82.2	60.8	88.0	12.0	0

Reaction conditions: ethylbenzene, catalyst, 0.05 g; 2.0 mmol; TBHP, 2.0 mmol; CO$_2$ pressure, 150 bar; reaction temperature, 120 °C; reaction time, 8 h. Legends: Ac; Acetophenone, Bd; Benzaldehyde, Ba; Benzoic acid.

[a] Oxidant: H_2O_2.
[b] Ethylbenzene to TBHP: 1:5.
[c] Ethylbenzene to TBHP: 1:3.
[d] Reaction time: 4 h.
[e] Reaction time: 24 h.
[f] Reflux condition for 12 h.
[g] For the six run (after 48 h).
[h] For the nine run (after 72 h).
[i] TON, turn over number, moles of substrate converted per mole of metal.

Scheme 2. Mn-catalyzed oxidation of ethylbenzene to acetophenone in *sc*CO$_2$.

reached a maximum. A large excess of TBHP (3 and 5 times that of substrate, Table 2, entries 8 and 9) afforded good conversion. All catalysts were found to be highly reactive and selective for the oxidation of ethylbenzene, although the fact that the catalytic activity of Mn catalysts immobilized on the functionalized Si/Al mixed-oxide varied significantly probably depends on their structures. The catalyst prepared with 2-AE-3-APTMS showed the best performance. As can be seen from Table 2, compared with those containing 3-APTES, the reaction with Si/Al-*pr*-NH-*et*-N=methyl-2-pyridylketone-Mn as catalysts provides a very high conversion of 83% and a very high selectivity for acetophenone (86%). This difference probably arises due to the surface properties of the modified Si/Al mixed-oxides containing two spacers. On the other hand, the increased conversion and selectivity may be due to the improved surface hydrophobicity of the Si/Al mixed-oxide modified with 2-AE-3-APTMS, the reduced interaction of the immobilized Mn catalysts with the host support and the greater flexibility of the active sites, which makes them more accessible to the substrate in *sc*CO$_2$.

3.1.2. The effect of immobilized ligands on Mn activity

Besides coordinating to a Schiff-base ligand, the Mn catalysts can also interact with the surface Si—OH and Al—OH groups of the Si/Al mixed-oxide. In light of this, the catalytic ability of a non-functionalized Si/Al mixed-oxide with adsorbed manganese acetate was also tested. The conversion of ethylbenzene in this case was almost 0%, thus indicating that the Mn ions absorbed on the surface of the mixed oxide did not catalyze the oxidation of ethylbenzene with TBHP. These findings suggest that catalytic oxidation only occurs when the Mn catalysts are chemically immobilized on Schiff-base ligands. Thus, in light of the different catalytic activities (see Table 2, entry 5), the Mn catalyst immobilized on Si/Al-*pr*-NH-*et*-N=methyl-2-pyridylketone was selected for further studies to determine the effect of various other reaction parameters.

3.1.3. The effect of CO$_2$ pressure

To gain an insight into the role of CO$_2$, an experiment was performed under similar reaction conditions but without CO$_2$ (Table 2; entry 13). Compared with the results without CO$_2$, the catalyst gave a higher conversion of ethylbenzene in the presence of CO$_2$, thus highlighting that this system promotes the oxidation of ethylbenzene to acetophenone. The conversion and selectivity increased from 41% to 84% and 72% to 86.0%, respectively, upon increasing the CO$_2$ pressure (50–150 bar), then decreased to 80.0% and 81.9%, respectively, at 200 bar (Fig. 2). This is due to the fact that the solvent power of CO$_2$ increases upon increasing the pressure from 50 to 150 bar, thereby increasing the reagent concentration in *sc*CO$_2$. However, a further pressure increase (150–300 bar) at constant volume forces more CO$_2$ molecules between the reagent molecules, thus mimicking the enhanced dilution effects of conventional solvents and decreasing both conversion and selectivity. Surprisingly, the selectivity for benzoic acid decreased with increasing CO$_2$ pressure (50–150 bar) possibly as a result of the favorable physicochemical properties of *sc*CO$_2$ in the reaction system preventing further oxidation of benzaldehyde to benzoic acid.

Benzaldehyde may form upon cleavage of the C—C bond, whereas benzoic acid is formed by oxidation of benzaldehyde.

3.1.4. The effect of time

The catalytic performance of the Si/Al-*pr*-NH-*et*-N=methyl-2-pyridylketone-Mn catalyst as a function of reaction time was investigated at 120 °C in *sc*CO$_2$ (150 bar) and the results are shown in Table 2 and Fig. 3. The selectivity for acetophenone initially increased sharply in the period 0–8 h and then reached a plateau. This indicates that the rate of side reactions gradually decreased
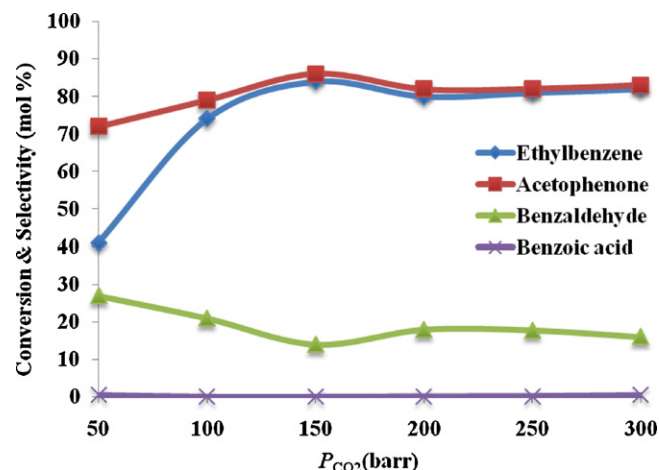

Fig. 2. Influence of CO$_2$ pressure on the conversion and selectivity of ethylbenzene oxidation with TBHP in the presence of Si/Al-*pr*-NH-*et*-N=methyl-2-pyridylketone-Mn. *Reaction conditions*: ethylbenzene: 2.0 mmol; catalyst: 0.05 g; TBHP: 2.0 mmol; reaction temp.: 120 °C; reaction time: 8 h.
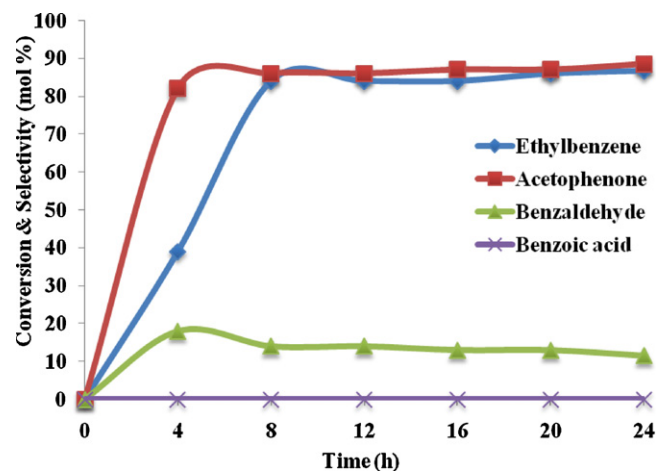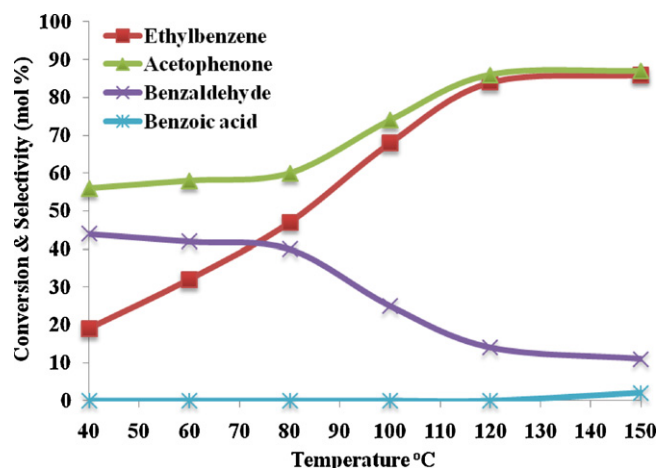

Fig. 3. The dependence of conversion and product selectivity on reaction time for the oxidation of ethylbenzene with TBHP in the presence of Si/Al-*pr*-NH-*et*-N=methyl-2-pyridylketone-Mn catalyst. *Reaction conditions*: ethylbenzene: 2.0 mmol; catalyst: 0.05 g; TBHP: 2.0 mmol; CO$_2$ pressure: 150 bar; reaction temp.: 120 °C.

Fig. 4. The effect of reaction temperature on the catalytic oxidation of ethylbenzene with TBHP in the presence of Si/Al-*pr*-NH-*et*-N=methyl-2-pyridylketone-Mn catalyst. *Reaction conditions*: ethylbenzene: 2.0 mmol; catalyst: 0.05 g; TBHP: 2.0 mmol; CO_2 pressure: 150 bar; reaction time: 8 h.

as the reaction progressed, thus leading to a higher selectivity for acetophenone. After 8 h, the acetophenone selectivity remained unaltered up to 24 h with respect to that for the other products.

3.1.5. The effect of temperature

The effect of temperature on the catalytic activity of Si/Al-*pr*-NH-*et*-N=methyl-2-pyridylketone-Mn for the oxidation of ethylbenzene with TBHP was assessed at 150 bar for 8 h (Fig. 4). Thus, increasing the temperature from 40 to 150 °C resulted in a higher conversion (19–86%) and selectivity for acetophenone (56–87%) and a dramatic decrease in benzaldehyde selectivity from 44% to 11%. These results indicate that raising the temperature favors the selective oxidation of ethylbenzene to acetophenone and reduces the conversion of ethylbenzene to benzaldehyde.
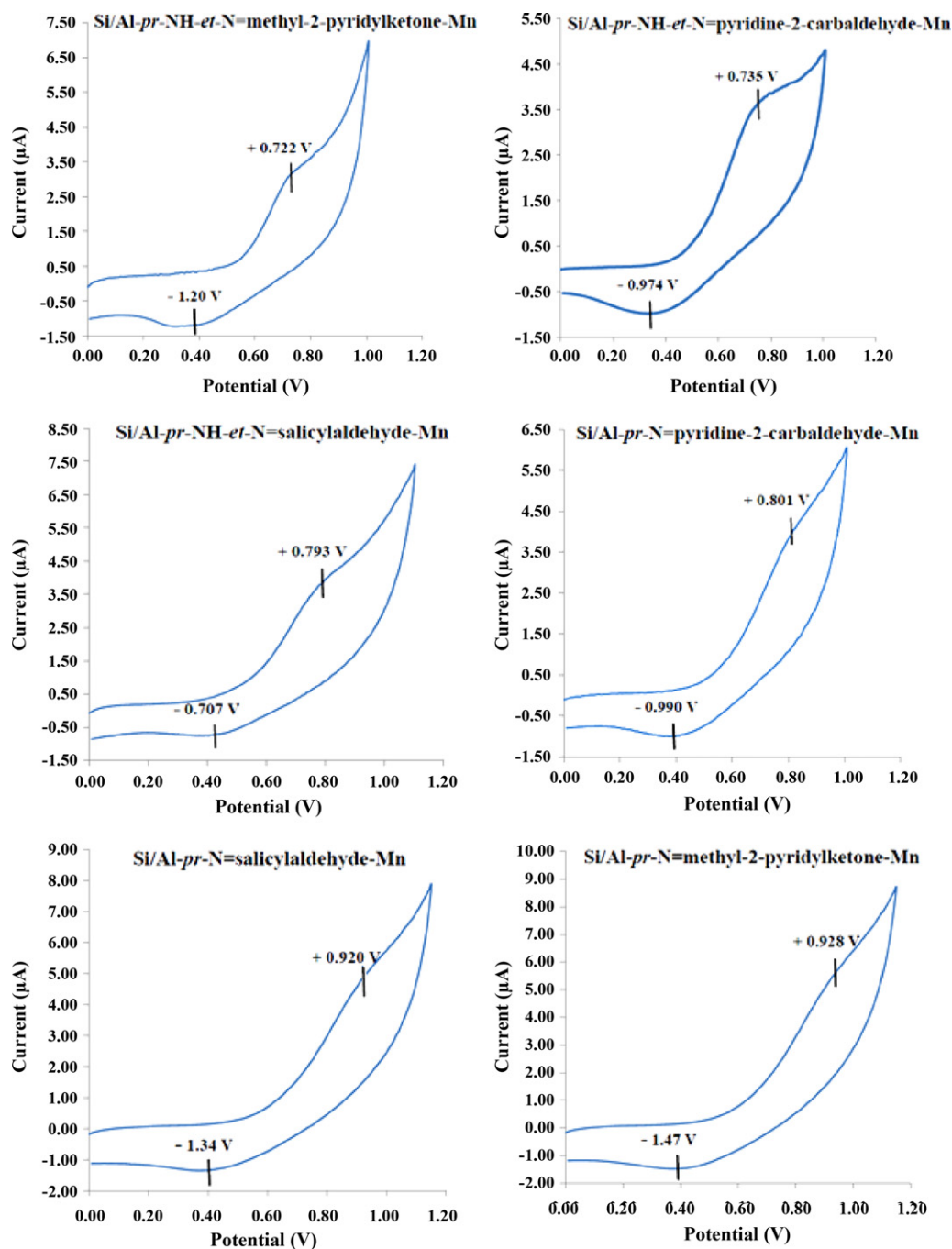
3.1.6. Cyclic test and catalyst stability

A successful Mn catalyst immobilization strategy necessarily involves a high immobilization efficiency and the resulting material must be stable under the experimental conditions. As a result, and to confirm the truly heterogeneous nature of the immobilized Mn catalysts for oxidation of ethylbenzene with TBHP, the Si/Al-*pr*-NH-*et*-N=methyl-2-pyridylketone-Mn catalyst was reused several times under the same reaction conditions after separation from the reaction mixture by centrifugation and washing several times. The results are presented in Table 2, which shows that the selectivity of the recycled catalyst remained almost unchanged after three cycles, although the catalytic activity (Table 2, entries 14 and 15) decreased gradually. Oxidation in the liquid phase with organic hydroperoxides or even H_2O_2 often results in catalyst leaching from the support, thus leading to some doubts regarding the true nature of the catalytic reaction (homogeneous or heterogeneous). To resolve these doubts, the oxidation reaction was cooled after each run (8 h) and, after separating the solid catalyst, the solution was analyzed for the presence of manganese. This AAS-based analysis showed that no manganese could be detected in the solution. In light of the reduced activity of the catalyst after each use, we conclude that most of the catalytic activity can still be attributed to heterogeneous catalysis and that any leached metal is deposited on the surface of the support, where it plays no active role in the oxidation reaction.

3.2. Electrochemical study

As a follow-up to this study, we used electrochemical methods to study the rate of electron transfer between the Mn catalysts as a higher rate of electron transfer ensures a better catalytic role in the redox reaction [32]. Indeed, it is well known in the field of coordination chemistry (i.e., in homogeneous media) that the redox potentials of couples involving transition metal catalysts depend on the nature of the ligands in the coordination sphere [33–35]. We therefore used electrochemical methods such as CV and EIS to study the electrochemical behavior of the synesized catalysts and to compare the dependence of the catalytic activity of the immobilized Mn catalysts on the electrochemical data obtained.

Fig. 5 shows the cyclic voltammograms obtained for various Mn catalysts in 0.04 mol/dm³ universal buffer at pH 7.0. All voltammograms exhibit a quasi-reversible anodic peak (E_{pa}) and the corresponding cathodic peak (E_{pc}) vs. Ag|AgCl|KCl$_{sat}$, which was used as reference electrode, for the Mn^{4+}/Mn^{3+} redox couple. As would be expected, the SiO$_2$/Al$_2$O$_3$ mixed-oxide and Mn-SiO$_2$-Al$_2$O$_3$ did not show any electrochemical activity. The shift in the oxidation potential for the various immobilized Mn catalysts, from low potential to high potential, increased in the order Si/Al-*pr*-NH-*et*-N=methyl-2-pyridylketone-Mn (E_{pa} = 0.722) < Si/Al-*pr*-NH-*et*-N=pyridine-2-carbaldehyde-Mn (E_{pa} = 0.737) < Si/Al-*pr*-NH-*et*-N=salicylaldehyde-Mn (E_{pa} = 0.793) < Si/Al-*pr*-N=pyridine-2-carbaldehyde-Mn (E_{pa} = 0.801) < Si/Al-*pr*-N=salicylaldehyde-Mn (E_{pa} = 0.920) < Si/Al-*pr*-N=methyl-2-pyridylketone-Mn (E_{pa} = 0.928). The electrochemical oxidation data correlate well with the conversion of ethylbenzene (see Table 2). Moreover, the results of the electrochemical measurements indicate that the oxidation of manganese takes place at lower potentials when the Mn catalyst is anchored to the SiO$_2$/Al$_2$O$_3$ mixed-oxide by 2-AE-3-APTMS than by 3-APTES. As discussed above, the voltammograms of the SiO$_2$/Al$_2$O$_3$ mixed-oxide modified with 2-AE-3-APTMS indicate an easily oxidizable environment, in accordance with the catalytic results (selectivity for acetophenone and conversion of ethylbenzene) and the lack of a close correlation with the selectivity data for the catalysts (see Table 2). Furthermore, the electrochemical results show that the anodic potential for the oxidation of Si/Al-*pr*-NH-*et*-N=methyl-2-pyridylketone-Mn is lower than those for all the other catalysts. This result is in accordance with the conversion of ethylbenzene, as a lower oxidation potential for the catalyst leads to a higher conversion and selectivity than for the other catalysts.
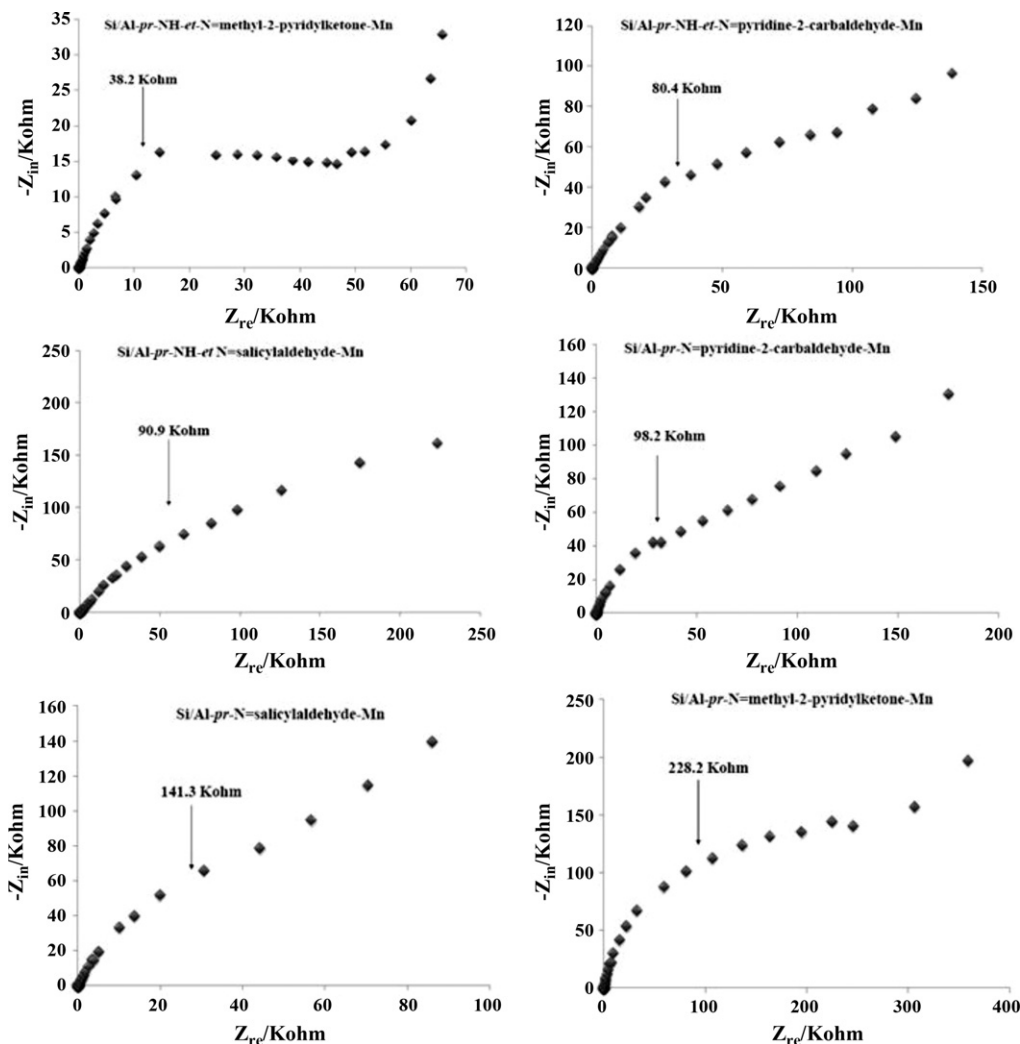
EIS, which is known to be a powerful electrochemical technique for characterizing and determining kinetic parameters such as charge-transfer resistance (R_{ct}) and solution resistance (R_s) of immobilized catalysts, was also used to investigate the oxidation ability of the Mn catalysts at the surface of a multi-walled carbon nanotube paste electrode (MWCNTPE). Figs. 6 and 7 present Nyquist diagrams and Bode plots for the imaginary impedance (Z_{im}) vs. the real impedance (Z_{re}) of the EIS obtained at a dc-offset of 0.70 V for the Mn catalysts immobilized on the functionalized SiO$_2$/Al$_2$O$_3$ mixed-oxide in universal buffer (pH 7.0). In the presence of the Mn catalysts, the Nyquist diagram comprises a depressed semicircle at high frequencies due to the combination of charge-transfer resistance for electro-oxidation of these compounds and the double-layer capacitance (C_d), which is generally a function of potential, followed by a straight line with a slope of nearly 45°. The latter is due to the occurrence of a diffusion-based mass-transport process [36]. The equivalent circuit compatible with the recorded Nyquist diagram is depicted in Scheme 3. In this circuit, R_s, CPE, and R_{ct} represent solution resistance, a constant phase element corresponding to the double-layer capacitance, and the charge-transfer resistance associated with the oxidation of

Fig. 5. Cyclic voltammograms for several Mn catalysts immobilized on the functionalized SiO_2/Al_2O_3 mixed-oxide via two different linkers at the surface of a multi-walled carbon nanotube paste electrode.

low-valent Mn species, respectively, and W is a finite-length Warburg short-circuit term coupled to R_{ct}, which accounts for the Nernstian diffusion. The results show that the value of R_{ct} differs depending on the Mn catalyst. The charge-transfer resistance is related to the ability of a compound to take part in an electro-oxidation reaction [37]. Furthermore, the charge-transfer resistance of the electrode reaction in the aforementioned circuits is the only circuit element that has a simple physical meaning, describing how fast the rate of charge transfer during electro-oxidation of the Mn nanocatalysts changes with the electrode potential. Consequently, compounds with a high charge-transfer resistance are less active due to the inability of the compound to oxidize the reagent to the desired product. We therefore

determined the value of R_{ct} for all the heterogeneous Mn catalysts studied in order to gain a better understanding of their oxidation activity. The charge-transfer resistance of the Mn catalysts follows the order Si/Al-*pr*-NH-*et*-N=methyl-2-pyridylketone-Mn (R_{ct} = 38.2 kΩ) < Si/Al-*pr*-NH-*et*-N=pyridine-2-carbaldehyde-Mn (R_{ct} = 80.4 kΩ) < Si/Al-*pr*-NH-*et*-N=salicylaldehyde-Mn (R_{ct} = 90.9 kΩ) < Si/Al-*pr*-N=pyridine-2-carbaldehyde-Mn (R_{ct} = 98.2 kΩ) < Si/Al-*pr*-N=salicylaldehyde-Mn (R_{ct} = 143.1 kΩ) < Si/Al-*pr*-N=methyl-2-pyridylketone-Mn (R_{ct} = 228.2 kΩ). In light of the above observations, in other words the decreasing charge-transfer resistance and the influence of the charge-transfer resistance on the selectivity of the catalysts, we propose that the Mn catalysts immobilized on the modified Si/Al mixed oxide via 2-AE-3-APTMS
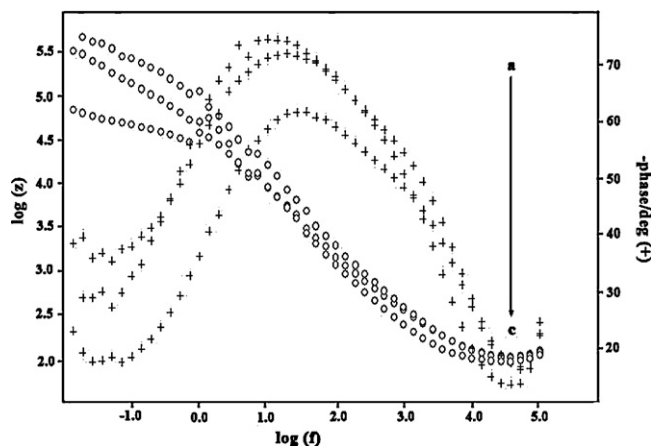
Fig. 6. Nyquist diagrams showing the imaginary impedance (Z_{im}) vs. the real impedance (Z_{re}) of the EIS obtained using a multi-walled carbon nanotube electrode recorded for Mn complexes immobilized on the functionalized SiO_2/Al_2O_3 mixed-oxide via two different linkers.
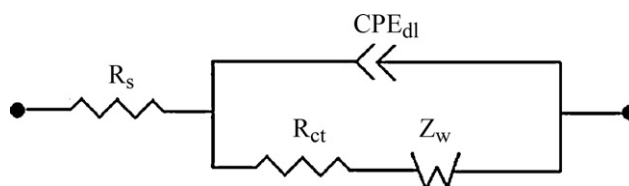
have a lower R_{ct} than 3-APTES. This may be due to the flexibility of the 2-AE-3-APTMS, which would result in a decreased interaction with the Si/Al mixed-oxide support [38]. Such a decreased interaction would decrease R_{ct} and increase the efficacy of the corresponding catalysts in the electro-oxidation reaction.
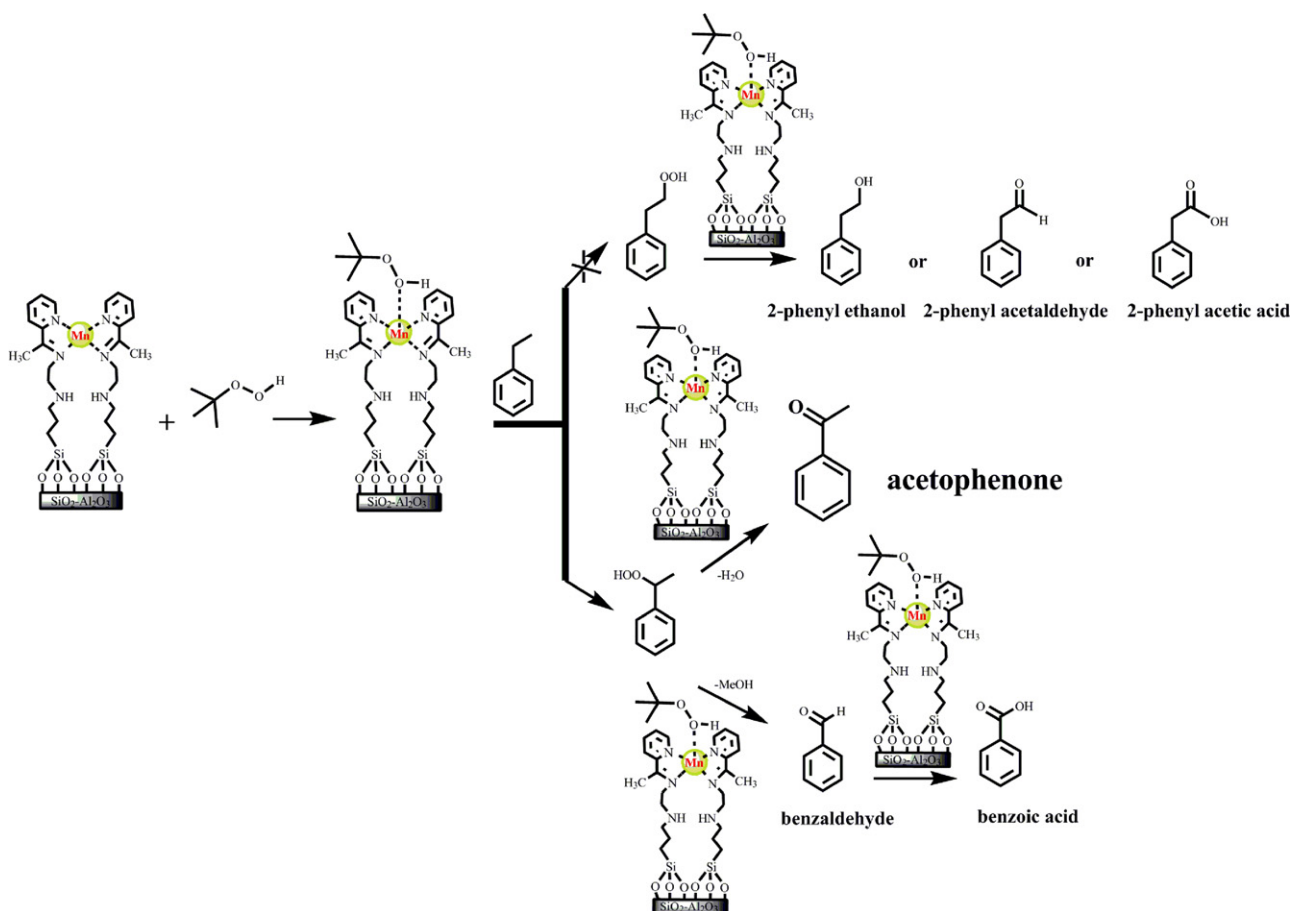
It was very interesting to note that the efficiency of the Mn catalysts immobilized on the functionalized SiO_2/Al_2O_3 mixed-oxide for the selective oxidation of ethylbenzene to acetophenone with TBHP is closely related to the E_{pa} and charge-transfer resistance (R_{ct}) obtained by CV and EIS, respectively. Therefore, in light of the above discussion, the greater activity of Si/Al-*pr*-NH-*et*-N=methyl-2-pyridylketone-Mn clearly arises from the presence of an electron-donating ligand (pyridine group), which facilitates electron transfer and probably increases the electron density of the manganese sites of the catalyst, thereby leading to a significant increase in conversion and selectivity.

Fig. 7. Bode plots for the EIS obtained using a multi-walled carbon nanotube electrode recorded for: (a) Si/Al-*pr*-NH-*et*-N=pyridine-2-carbaldehyde-Mn; (b) Si/Al-*pr*-NH-*et*-N=salicylaldehyde-Mn; (c) Si/Al-*pr*-N=salicylaldehyde-Mn.

Scheme 3. The equivalent circuit compatible with the Nyquist diagram recorded.

Scheme 4. Proposed mechanism for the oxidation of ethylbenzene with *tert*-butyl hydroperoxide in the presence of Si/Al-*pr*-NH-*et*-N=methyl-2-pyridylketone-Mn in *sc*CO$_2$.

3.3. Proposed mechanism

The mechanism for the oxidation of ethylbenzene with TBHP in the presence of Si/Al-*pr*-NH-*et*-N=methyl-2-pyridylketone-Mn is proposed to occur as shown in Scheme 4. Oxidation of ethylbenzene with TBHP follows a free-radical mechanism to initially yield ethylbenzene hydroperoxide [39]. TBHP is activated upon coordination to the immobilized Mn nanocatalyst, whereupon the activated oxygen of co-coordinated TBHP reacts with ethylbenzene to yield the products. No other products (2-phenylethanol, 2-phenylacetaldehyde and 2-phenylacetic acid) were detected in the reaction mixture by GC–MS (disfavored path in Scheme 4). As shown in Scheme 4, the intermediate ethylbenzene hydroperoxide can react in two ways to form two different products, namely acetophenone or benzaldehyde, although the formation of benzoic acid as a result of over-oxidation of benzaldehyde cannot be excluded.

4. Conclusions

We have described a series of new, easily recoverable and efficient Mn catalysts for the oxidation of ethylbenzene with TBHP at 120 °C in *sc*CO$_2$ medium. We have also demonstrated that the combination of an organic ligand and the SiO$_2$/Al$_2$O$_3$ mixed-oxide results in an interesting synergistic effect that leads to enhanced activity and selectivity, prevents precipitation of the Mn catalysts, and leads to a catalyst that is active under CO$_2$ pressure. Among the compounds investigated, the Mn catalyst immobilized on Si/Al-*pr*-NH-*et*-N=methyl-2-pyridylketone was found to be the optimal heterogeneous catalyst system for the selective oxidation of ethylbenzene. Indeed, a high conversion (84%) and excellent selectivity (up to 86%) were obtained under mild *sc*CO$_2$ reaction conditions with a substrate-to-oxidant ratio of one. The relationship between the efficiency of the prepared catalysts for ethylbenzene oxidation and their redox potential and charge-transfer resistance has been demonstrated by cyclic voltammetry and electrochemical impedance spectroscopy, respectively. Further applications of this new approach for other transition metal-based nanocatalysts are currently being studied.

References

[1] G.A. Olah, Friedel-Crafts and Related Reactions, Wiley–Interscience, New York, 1963.
[2] B. Aikawa, R.C. Burk, B.B. Sitholé, Appl. Catal. B: Environ. 32 (2001) 269–280.
[3] A. Corma, H. Garcia, Chem. Rev. 102 (2002) 3837–3892.
[4] U.R. Pillai, E. Sahle-Demessie, D. Young, Appl. Catal. B: Environ. 43 (2003) 131–138.
[5] B. Kerler, R.E. Robinson, A.S. Borovik, B. Subramaniam, Appl. Catal. B: Environ. 49 (2004) 91–98.
[6] R.A. Lucky, P.A. Charpentier, Appl. Catal. B: Environ. 96 (2010) 516–523.
[7] L.B. Zhou, A. Akgerman, Ind. Eng. Chem. Res. 34 (1995) 1588–1595.
[8] C.T. Wang, R.J. Willey, Catal. Today 52 (1999) 83–89.
[9] G. Jenzer, D. Sueur, T. Mallat, A. Baiker, Chem. Commun. (2000) 2247–2248.
[10] M. Caravati, J.-D. Grunwaldt, A. Baiker, Phys. Chem. Chem. Phys. 7 (2005) 278–285.

[11] X. Wang, N.S. Venkataramanan, H. Kawanami, Y. Ikushima, Green Chem. 9 (2007) 1352–1355.
[12] R. Mello, A. Olmos, J. Parra-Carbonell, M.E. Gonzalez-Nunez, G. Asensio, Green Chem. 11 (2009) 994–999.
[13] T. Seki, A. Baiker, Chem. Rev. 109 (2009) 2409–2454.
[14] H. Jiang, L. Jia, J. Li, Green Chem. 2 (2000) 161–164.
[15] N. Theyssen, Z. Hou, W. Leitner, Chem.-Eur. J. 12 (2006) 3401–3409.
[16] R.L. Holliday, B.Y.M. Jong, J.W. Kolis, J. Supercrit. Fluids 12 (1998) 255–260.
[17] D.P. Kessissoglou, Coord. Chem. Rev. 185 (1999) 837–858.
[18] C. Guo, Q. Peng, Q. Liu, G. Jiang, J. Mol. Catal. A: Chem. 192 (2003) 295–302.
[19] K.M. Parida, S.S. Dash, J. Mol. Catal. A: Chem. 306 (2009) 54–61.
[20] R. Breinbauer, E.N. Jacobsen, Angew. Chem. Int. Ed. 39 (2000) 3604–3607.
[21] X. Yao, H. Chen, W. Lü, G. Pan, X. Hu, Z. Zheng, Tetrahedron Lett. 41 (2000) 10267–10271.
[22] J.M. Ready, E.N. Jacobsen, J. Am. Chem. Soc. 123 (2001) 2687–2688.
[23] M.R. Maurya, I. Jain, S.J.J. Titinchi, Appl. Catal. A: Gen. 249 (2003) 139–149.
[24] M. Kwon, G.-J. Kim, Catal. Today 87 (2003) 145–151.
[25] Ch. Hajji, S. Roller, M. Beigi, A. Liese, R. Haag, Adv. Synth. Catal. 348 (2006) 1760–1771.
[26] A. Bottcher, M.W. Grinstaff, J.A. Labinger, H.B. Gray, J. Mol. Catal. A: Chem. 113 (1996) 191–200.
[27] R.F. Davis, J.A. Pask, in: A.M. Alper (Ed.), "Mullite" in High Temperature Oxides Part I, Academic Press, UK, 1971, p. 37.
[28] M. Ghiaci, B. Rezaei, M. Arshadi, Sens. Actuators B 139 (2009) 494–500.
[29] M. Arshadi, M. Ghiaci, A.A. Ensafi, H. Karimi-Maleh, L. Suib, J. Mol. Catal. A. Chem. 338 (2011) 71–83.
[30] M. Arshadi, M. Ghiaci, Appl. Catal. A: Gen. 399 (2011) 75–86.
[31] M.J. Sabater, A. Corma, J.V. Folgado, H. Garcia, J. Phys. Org. Chem. 13 (2000) 57–62.
[32] L. Saikia, D. Srinivas, P. Ratnasamy, Microporous Mesoporous Mater. 104 (2007) 225–235.
[33] D.D. Perrin, Rev. Pure Appl. Chem. 9 (1959) 257–285.
[34] H.L.M. Van Gaal, J.G.M. Van der Linden, Coord. Chem. Rev. 47 (1982) 41–54.
[35] G. Lappin, Redox Mechanisms in Inorganic Chemistry, Ellis Horwood Limited, Chichester, England, 1994.
[36] H. Karimi-Maleh, A.A. Ensafi, A.R. Allafchian, J. Solid State Electrochem. 14 (2010) 9–15.
[37] A.J. Bard, L.R. Faulkner, Electrochemical Methods: Fundamentals and Applications, Wiley, New York, 2001.
[38] M.A. Ghanem, J.-M. Chretien, A. Pinczewska, J.D. Kilburn, P.N. Bartlett, J. Mater. Chem. 18 (2008) 4917–4927.
[39] J.D. Chen, R.A. Sheldon, J. Catal. 153 (1995) 1–8.